

The star cluster Collinder 232 in the Carina complex and its relation to Trumpler 14/16²

Giovanni Carraro^{1,2}, Martino Romaniello², Paolo Ventura³, and Ferdinando Patat²

¹ Dipartimento di Astronomia, Università di Padova, vicolo dell'Osservatorio 2, I-35122, Padova, Italy

² European Southern Observatory, Karl-Schwarzschild-Str 2, D -85748 Garching b. München, Germany

³ Osservatorio Astronomico di Roma, Via di Frascati 33, I-00040, Monte Porzio Catone, Italy

Received September 2003; accepted

Abstract. In this paper we present and analyze new CCD UBVR I photometry down to $V = 21$ in the region of the young open cluster Collinder 232, located in the Carina spiral arm, and discuss its relationship to Trumpler 14 and Trumpler 16, the two most prominent young open clusters located in the core of NGC 3372 (the Carina Nebula). First of all we study the extinction pattern in the region. We find that the total to selective absorption ratio R_V differs from cluster to cluster, being $3:48 \pm 0:11$, $4:16 \pm 0:07$ and $3:73 \pm 0:01$ for Trumpler 16, Trumpler 14 and Collinder 232, respectively. Then we derive individual reddenings and intrinsic colours and magnitudes using the method devised by Romaniello et al. (2002). Ages, age spreads and distances are then estimated by comparing the Colour Magnitude Diagrams and the Hertzsprung-Russell diagram with post and pre-main sequence tracks and isochrones. We find that Trumpler 14 and Collinder 232 lie at the same distance from the Sun (about 2.5 kpc), whereas Trumpler 16 lies much further out, at about 4 kpc from the Sun. As for the age, we find that Trumpler 16 is older than both Trumpler 14 and Collinder 232. For all the clusters we indicate the existence of a significant age dispersion, whose precise value is hampered by our inability to properly distinguish members from non-members. We finally suggest that Collinder 232 is a physical aggregate and provide estimates of its basic parameters.

Key words. Photometry : optical | Open clusters and associations : Collinder 232 : individual : Trumpler 14 : individual : Trumpler 16 : individual

1. Introduction

Aiming at providing a homogeneous photometric database for all the open clusters located in the Carina complex (Feinstein 1995, Smith et al 2001), we have carried out an observational program which resulted in the multicolor UBVR I photometry of 12 star clusters in a $2^\circ \times 2^\circ$ region around Carina. We already reported on some of these clusters in a series of papers (Carraro et al 2001, Patat & Carraro 2001, Carraro & Patat 2001, Carraro 2002, Baume et al. 2003).

Here we concentrate on Collinder 232 (Collinder 1931) and on the very well studied Trumpler 14 and Trumpler 16 clusters close to Carina (Trumpler 1930). Collinder 232 ($\alpha = 10:44:48.0$, $\delta = -59:34:00.0$, $l = 187.51$, $b = -0.54$; J2000.0) is located near the northern edge of the Great Carina Nebula, about 6° above Carina.

Send *o* print requests to: Giovanni Carraro (giovanni.carraro@unipd.it)

² Based on observations taken at ESO La Silla. Tables 1 and 2 are available only in electronic form at the CDS via anonymous ftp to cdsarc.u-strasbg.fr (130.79.128.5) or via <http://cdsweb.u-strasbg.fr/cgi-bin/qcat?J/A+A/>

Unlike the other clusters in this region (Trumpler 14, 15 and 16), which appear rather compact on sky maps, Collinder 232 is more sparse and less rich in stars. Although several observations have been carried out in the past in this region, a systematic and detailed study of this cluster is still missing. Moreover, we analyze the data for one field centered on Trumpler 14, and 3 fields in the region of Trumpler 16, aiming at investigating the relationship between Collinder 232 and these two clusters, in order to establish whether or not they lie at the same distance from the Sun, whether or not they are coeval, and, finally, whether or not they are individual objects. These facts, in turn, are crucial in order to understand the Star Formation (SF) history of the region. These questions have already been addressed many times in the past, often leading to contradictory results. A very detailed study of Trumpler 14 has been conducted by Vazquez et al (1996), whereas a recent study on Trumpler 16 and Trumpler 14 has been presented by DeGolia-Eastwood et al (2001), whom the reader is referred to for further details. This latter study shows that the two clusters lie at the same distance and are

almost coeval. However the result is hampered by the assumption that the reddening law is normal in the entire region, although previous studies – like for instance Vazquez et al. (1996) – had convincingly shown that at least in the region of Trumpler 14 the extinction is anomalous.

To briefly summarize the current understanding, we follow Walborn (1995), who provided a nice review of the present status of our knowledge of the region around Carina:

- Trumpler 14 seems to be younger than Trumpler 16;
- both clusters lie at the same distance from the Sun;
- Collinder 232 is not a physical system, but contains stars which belong to Trumpler 14 or Trumpler 16;
- Collinder 228 is part of Trumpler 16;
- the extinction toward this region is still very controversial;
- If a difference in R_V exists between Trumpler 14 and 16, in the sense that $R_V(\text{Tr14}) = R_V(\text{Tr16}) + 1$, there would be no need for either a distance or age difference between the two clusters.

This picture is essentially confirmed by the recent paper by Tapia et al. (2003).

In this paper we present new UBVRI deep CCD photometry for all the 3 clusters, aiming at deriving homogeneous estimates for their fundamental parameters, like distance, age and interstellar absorption.

The layout of the paper is as follows: Section 2 presents in details the data acquisition and reduction. In Section 3 we discuss previous investigations of Collinder 232; in Section 4 we present our data and compare our photometry with previous ones. In Section 5 we briefly summarize Trumpler 14 and 16 properties, and compare our photometry for these clusters with data available from the literature. In Section 6 we critically discuss the extinction pattern in the direction of the Carina nebula and derive the individual reddening and membership of stars in Collinder 232, Trumpler 14 and 16. Section 7 is dedicated to derive estimates for Collinder 232, Trumpler 14 and Trumpler 16 ages and distances. Then, in Section 8 we discuss the mutual relationship between the 3 clusters and re-analyse the SF history in the Carina region, providing the basic conclusions of this investigation.

2. Observations and Data Reduction

Observations were conducted at La Silla on April 14-16, 1996, using the imaging camera (equipped with a TK coated 512 × 512 pixels CCD # 33) mounted at the Cassegrain focus of the 0.92m ESO (Dutch) telescope. The scale on the chip is $0^{\text{m}}.44 \text{ pix}^{-1}$ and the array covers about $3^{\text{m}}.3 \times 3^{\text{m}}.3$ on the sky. Due to the projected diameter of the objects and the relatively small field of view, it was necessary to observe two overlapping fields for Collinder 232. The nights were photometric

with an average seeing of 1.6 arcsec. To allow for a proper photometric calibration and to assess the night quality, the standard fields RU 149, PG 1657, SA 109 and SA 110 (Landolt 1992) were monitored each night. Finally, a series of field frames on the twilight sky were taken. The scientific exposures have been flat and bias corrected by means of standard routines within IRAF¹. Further reductions were performed using the DAOPHOT-ALLSTAR packages (Stetson 1991) in the IRAF environment. Some details of the observations are given in the log-book in Table 1 and 2.

Moreover in the night of April 16, 1996 we observed 1 field centered in Trumpler 14, and 3 overlapping fields in the region of Trumpler 16. The basic information on these observations are reported in Table 2, whereas the covered regions are shown in Fig. 1, which reports a DSS image² of a $20^{\text{m}} \times 20^{\text{m}}$ region around Carina.

The transformation from instrumental magnitudes to the standard Kron-Cousins system was obtained with expressions of the form

$$M_i = m_i + z p_i + \epsilon_i (M_i - M_j) - k_{iz} \quad (1)$$

where M_i , m_i , $z p_i$, ϵ_i and k_i are the calibrated magnitude, instrumental magnitude, zero point, colour term and extinction coefficient for the i th passband and z is the airmass. The transformation requires of course the knowledge of the reference colour ($M_i - M_j$), which is easily computed from the instrumental magnitudes through the following relation:

$$(M_i - M_j) = \frac{m_i - m_j + z p_i - z p_j - (k_i - k_j) z}{\epsilon_{ij}} \quad (2)$$

where we have set $\epsilon_{ij} = 1 - \epsilon_i + \epsilon_j$. If m_i , $z p_i$, ϵ_i and k_i are the RMS errors on the instrumental magnitude, zero point, colour term and extinction coefficient for the i th passband, formal uncertainties on calibrated colors are then obtained propagating the various errors through Eq. 2 as follows:

$$\sigma_{(M_i - M_j)}^2 = \frac{\sigma_{m;ij}^2 + \sigma_{ps;ij}^2 + (M_i - M_j)^2 \sigma_{\epsilon;ij}^2}{\epsilon_{ij}^2} \quad (3)$$

For sake of simplicity, we have set $\sigma_{m;ij}^2 = \sigma_{m_i}^2 + \sigma_{m_j}^2$, $\sigma_{\epsilon;ij}^2 = \sigma_{\epsilon_i}^2 + \sigma_{\epsilon_j}^2$ and $\sigma_{ps;ij}^2 = \sigma_{z p_i}^2 + \sigma_{z p_j}^2 + z^2 \sigma_{k;ij}^2$.

Finally, the RMS uncertainties on the calibrated magnitudes are given by:

$$\sigma_{M_i}^2 = \sigma_{m_i}^2 + \sigma_{ps_i}^2 + (M_i - M_j)^2 \sigma_{\epsilon_i}^2 + \sigma_{\epsilon_i}^2 \sigma_{(M_i - M_j)}^2 \quad (4)$$

where we have neglected the error on z and assumed that the images in different passbands have been obtained at very similar airmass, as it was in fact the case.

¹ IRAF is distributed by the National Optical Astronomy Observatories, which is operated by the Association of Universities for Research in Astronomy, Inc., under contract to the National Science Foundation.

² Digital Sky Survey, <http://archive.eso.org/dss/dss>

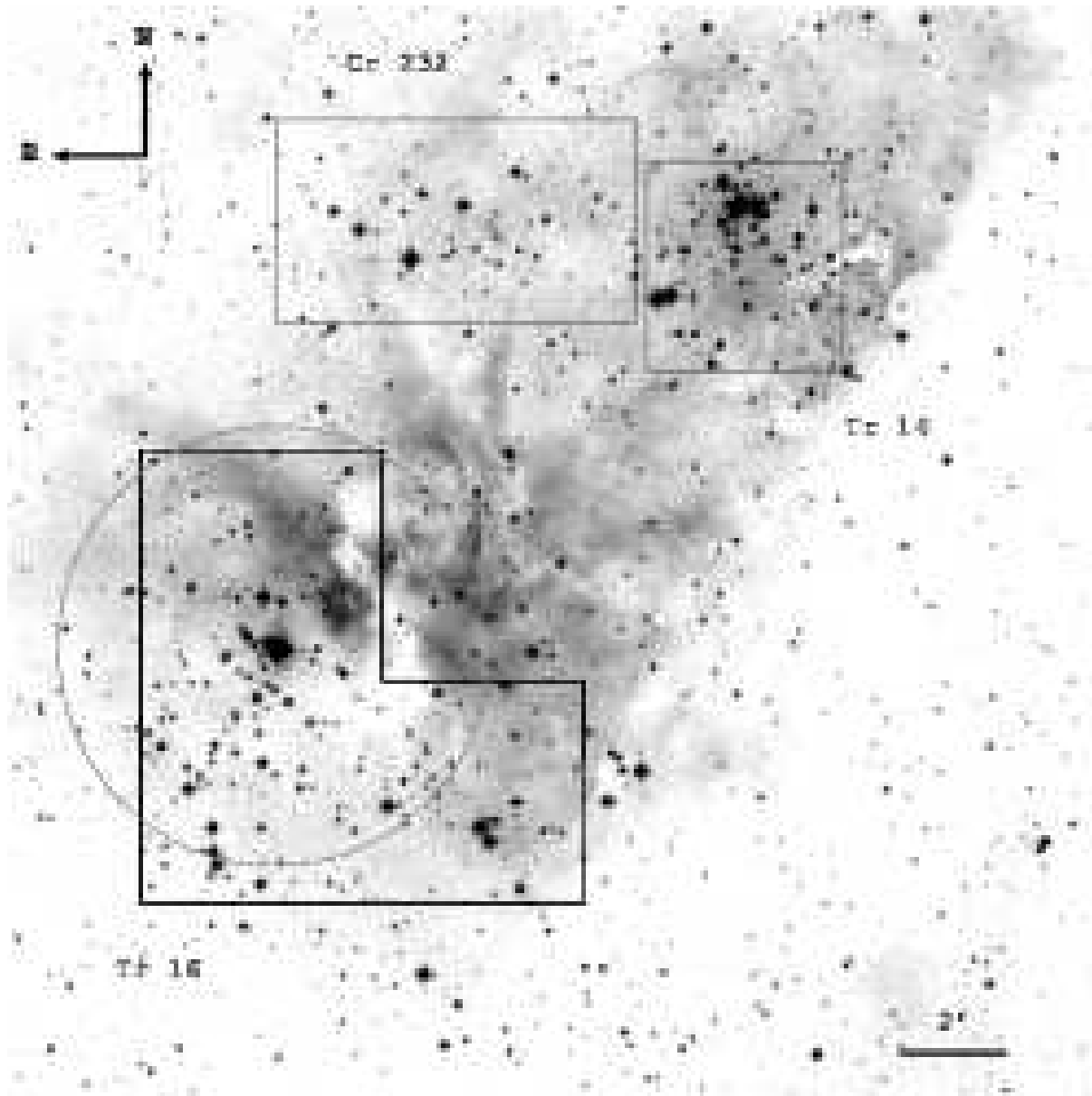


Fig. 1. A map of the observed regions around Collinder 232, Trumpler 14 and Trumpler 16. North is up, East to the left. The field is $20^{\circ} 20'$. The circle centered in Carina has a radius of $4'$ and encloses most of the stars believed to be associated with Trumpler 16. See text for more details.

Table 1. Journal of observations of Collinder 232 (April 14, 1996)

Table 2. Journal of observations of Trumpler 14 and Trumpler 16 (April 16, 1996)

Estimated uncertainties as a function of magnitude are reported in Tab. 4, from which it appears clearly that down to $V = 17$ they are dominated by the errors on the photometric solution, while at fainter magnitudes the contribution by the poissonian photon shot noise (estimated by DAOPHOT) becomes relevant.

3. Collinder 232: previous results

Collinder 232 was observed in the past several times due to its proximity to Carina and always in connection with Trumpler 16.

Massey & Johnson (1993) obtained Schmidt CCD photometry in UBV bands for about 50 stars down to $V = 14$ in their study of the young open clusters Trumpler 14 and 16.

Table 3. Average photometric coefficients obtained during April 13{16, 1996. ESO {Dutch 0.92m telescope, TK CCD # 33.

Filter	Ref. Color	zp				k	
U	(U - B)	19.85	0.02	0.095	0.020	0.46	0.02
B	(B - V)	21.93	0.01	0.079	0.010	0.27	0.02
V	(B - V)	22.19	0.01	0.030	0.006	0.12	0.02
R	(V - R)	22.18	0.01	0.025	0.014	0.09	0.02
I	(V - I)	21.11	0.01	0.062	0.006	0.06	0.02

Table 4. Global photometric RMS errors as a function of magnitude.

M ag	U	B	V	R	I
9{11	0.04	0.03	0.03	0.03	0.03
11{13	0.04	0.03	0.03	0.03	0.03
13{15	0.04	0.03	0.03	0.03	0.03
15{17	0.05	0.03	0.03	0.03	0.03
17{19	0.08	0.03	0.04	0.04	0.05
19{20	-	0.04	0.05	0.07	0.09
20{21	-	0.07	0.09	0.15	0.22
21{22	-	0.12	0.18	0.27	-

Similarly, Cudworth et al (1993) obtained photographic BV photometry for about 80 stars down to $V = 15.5$ in the region of Collinder 232 in their large astrometric survey of star clusters close to Carina. Cudworth et al (1993) selected cluster members on the basis of proper motions, and provided the first Color-Magnitude Diagram (CMD) of Collinder 232, although no estimates are given for the cluster fundamental parameters.

Tapia et al (1988) presented near-infrared JHKL photometry for 29 stars in Collinder 232. Nonetheless they associate Collinder 232 with Trumpler 16, and study the inter-stellar extinction toward these clusters considering them as a single system.

More recently, Tapia et al. (2003) obtained UBVR IJHK photometry in the field of Trumpler 14, 16 and Collinder 232, reaching approximately the same limiting magnitude. Finally, Levato & Malaraoda (1982) provide spectral classification for 4 stars in the field of Collinder 232.

4. The present study

We provide UBVR I photometry for 970 stars in a $6^{\circ}.3 \times 3^{\circ}.5$ region centered in Collinder 232. Limiting magnitudes (5 σ) are $U = 17$, $B = 22.3$, $V = 21.6$, $R = 20.9$ and $I = 20.6$. The region we sampled is shown in Fig. 1, where a V map is presented. In this map North is on the top, East to the left. Fig. 2 and Fig. 3 show the comparison of our photometry with the one of Massey & Johnson (40 common stars) and Cudworth et al (60 common stars), respectively.

In the case of Fig. 2 we notice that the agreement in magnitude is good up to $V = 12.0$, and below there is a large scatter. In the case of colour the same scatter is present, but there is no systematic difference. We

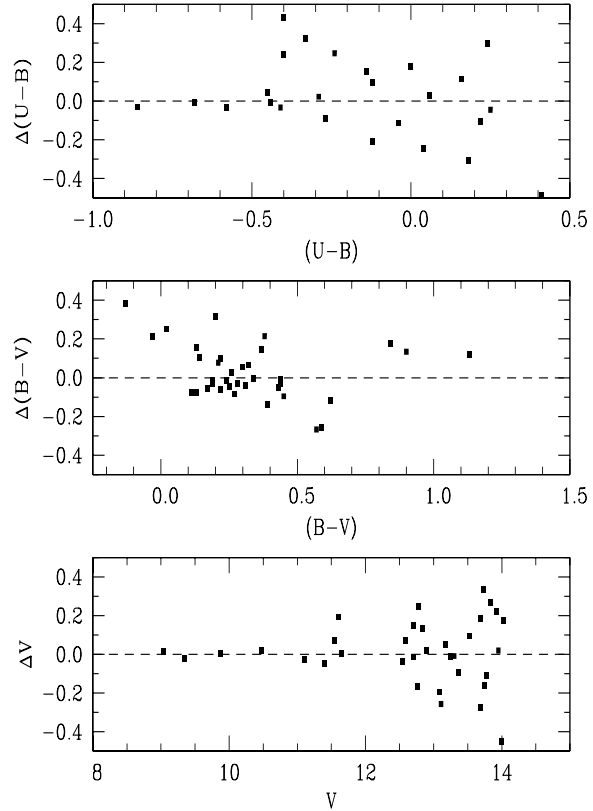


Fig. 2. A comparison of our photometry with Massey & Johnson (1993) study. The comparison is in the sense (this study - Massey & Johnson).

interpret the large scatter as due to Massey & Johnson (1993) photometry, which was obtained with a small Schmidt telescope and a CCD having a very large scale, almost $2''$ /pixels. Although the field is not particularly crowded, some stars are actually blended. Finally, the typical error at $V = 13.0 - 14.0$ is in the range 0.05-0.10 mag in the Massey & Johnson (1993) photometry, while in our case is 0.02-0.04 (Patat & Carraro 2001). By considering all the stars, we get

$$V_{CRVP} - V_{MJ} = 0.125 \pm 0.477$$

$$(B - V)_{CRVP} - (B - V)_{MJ} = 0.027 \pm 0.143$$

$$(U - B)_{CRVP} - (U - B)_{MJ} = 0.126 \pm 0.424$$

where the suffix CRVP refers to this study, and MJ to Massey & Johnson (1993). These numbers mirror the results of Fig. 2, emphasizing the existence of a large scatter. We stress however, that for V brighter than 11.5, the two photometries are consistent.

Some scatter is also visible in the comparison with Cudworth et al (1993) photographic photometry (Fig. 3).

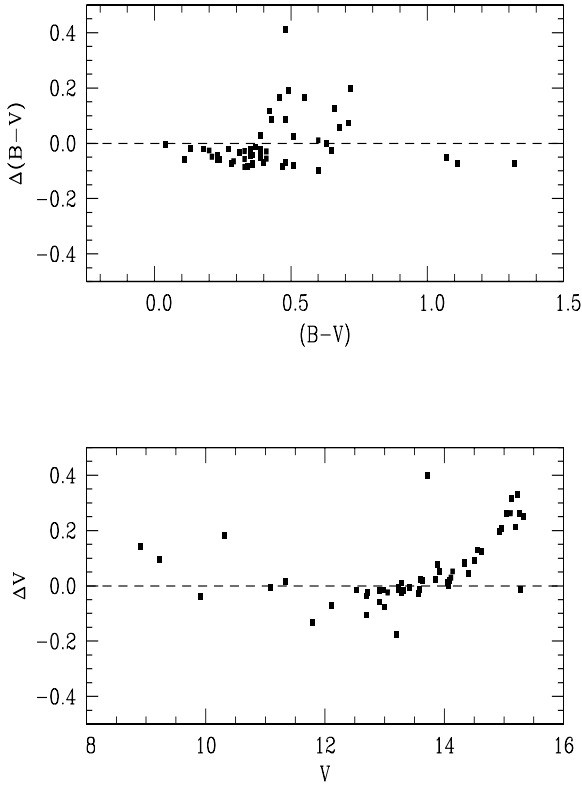


Fig. 3. A comparison of our photometry with Cudworth et al (1993) study. The comparison is in the sense (this study - Cudworth et al).

In this case the major source of errors is the poor precision of photographic photometry at the faint magnitude end, and the poor treatment of star blending in crowded regions. By considering only the stars brighter than $V = 14$ we get

$$V_{CRVP} - V_{CMDE} = 0:004 \quad 0:100$$

$$(B - V)_{CRVP} - (B - V)_{CMDE} = 0:049 \quad 0:024$$

which means that the two photometries are consistent up to this magnitude, and then the deviation becomes very large.

The CMDs from our photometry for all the measured stars is plotted in Fig. 4 in the planes $V - (B - V)$, $V - (V - I)$ and $V - (V - R)$. Our photometry reaches $V = 21$, although below $V = 18$ the scatter in color is quite large. This is mostly due to background star contamination, and only partially to photometric errors and the presence of unresolved binary systems, whose percentage in these clusters is around 30% (Levato et al 1990).

As for data completeness (V magnitude), we performed an analysis by using IRAF tasks ADDSTAR, which yields

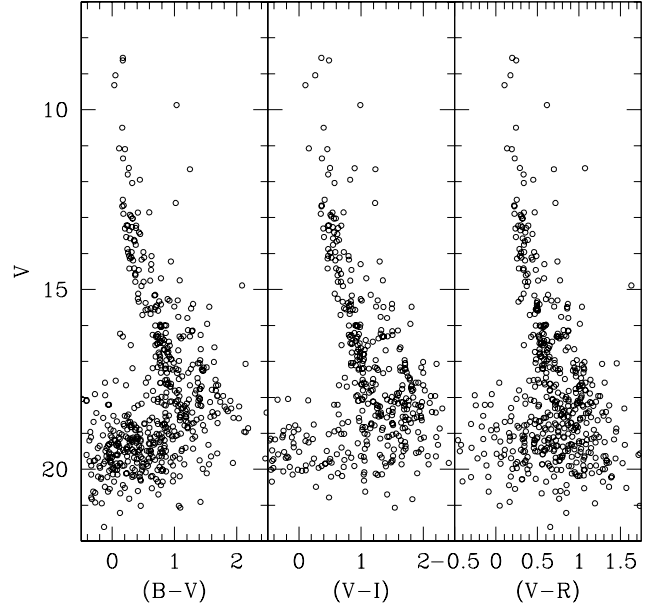


Fig. 4. The CMDs of Collinder 232 including all the detected stars.

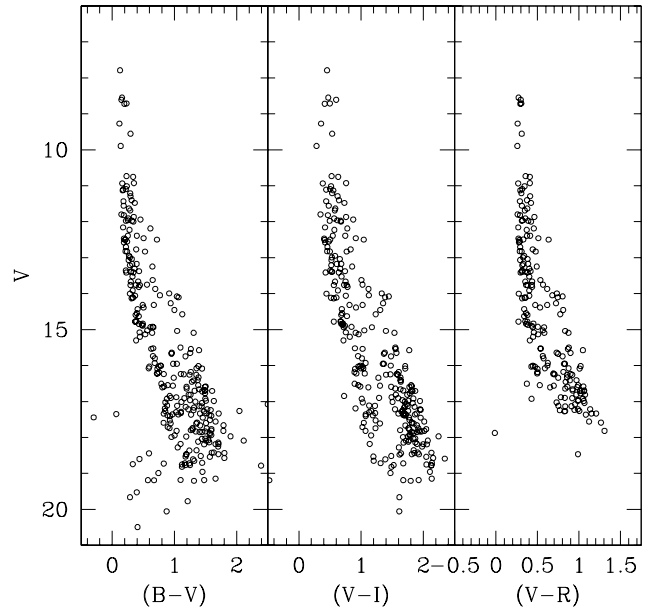


Fig. 5. The CMDs of Trumpler 14 including all the detected stars.

100% down to $V = 17.0$, 93% down to $V = 18.2$ and 57% down to $V = 19.0$.

5. Previous results for Trumpler 14 and 16

We report here photometry of a field centered on Trumpler 14, and 3 overlapping fields in the region of Trumpler 16 (see Fig. 1). In the case of Trumpler 16 the

Table 5. Extinction parameters of Trumpler 14 stars with near IR photometry and spectral classification.

ID	FMM 73.	Sp:Type	E(B-V)	R _V (i)	R _V (iii)	A _V (ii)	R _V (ii)
7	20	O6-V	0.596	3.67	3.46	1.79 0.05	3.00 0.13
10	21	O9-V	0.618	3.96	3.83	2.03 0.13	3.28 0.16
16	27	B1-V	0.521	4.45	4.51	2.05 0.21	3.94 0.29
27	18	B0-V	0.520	4.76	4.26	2.18 0.33	4.19 0.41
29	15	B7-V	0.477	4.56	4.42	1.91 0.41	4.00 0.48
31	26	B2-V	0.529	4.85	4.49	2.16 0.09	4.08 0.17
32	23	B1-V	0.571	4.24	3.79	1.96 0.24	3.44 0.37
35	22	B2-V	0.489	4.65	4.24	1.90 0.07	3.88 0.15
36	28	B2-V	0.606	4.23	2.90	2.17 0.13	3.59 0.22
42	12	B2-V	0.398	5.38	4.87	1.87 0.19	4.70 0.25

Table 6. Same as in Table 5, but for Collinder 232.

ID	FMM 73.	Sp:Type	E(B-V)	R _V (i)	R _V (iii)	A _V (ii)	R _V (ii)
1	HD 93160	O6.5-V	0.472	3.82	3.68	1.55 0.05	3.29 0.13
2	HD 93161	O6-III	0.470	4.12	3.90	1.63 0.13	3.47 0.16
6	31	B0-V	0.421	4.44	3.88	1.52 0.21	3.62 0.29

Table 7. Same as in Table 5, but for Trumpler 16.

ID	FMM 73.	Sp:Type	E(B-V)	R _V (i)	R _V (iii)	A _V (ii)	R _V (ii)
2	110	O7-V	0.606	4.35	4.10	2.22 0.05	3.67 0.13
3	34	O8.5-V	0.610	3.75	3.66	2.06 0.13	3.37 0.16
4	27	O4.5-V	0.606	4.19	4.07	2.26 0.21	3.73 0.29
5	1	O9.5-V	0.422	1.68	0.89	0.46 0.33	1.09 0.41
7	HD 93343	O8-V	0.508	4.37	4.10	1.97 0.41	3.89 0.48
8	9	O9.5-V	0.512	3.84	3.58	1.66 0.09	3.38 0.17
9	23	O7-V	0.633	2.74	2.42	3.44 0.24	2.63 0.37
12	3	O9-V	0.537	2.94	2.43	1.47 0.07	2.74 0.15
15	8	B1.5-V	0.427	3.54	3.22	1.50 0.13	3.51 0.22
16	2	B1.5-V	0.406	3.01	2.63	1.06 0.19	2.61 0.25
20	65	B1.5-V	0.409	4.56	4.24	1.59 0.07	2.89 0.15
22	22	O8.5-V	0.707	3.01	3.00	1.87 0.13	2.65 0.22
24	4	B2-V	0.497	4.61	4.38	1.99 0.19	4.00 0.25
25	12	B2-V	0.624	3.91	4.01	2.25 0.19	3.60 0.25

limiting magnitudes are $U = 19.9, B = 21.0, V = 20.6, R = 20.1$ and $I = 19.9$, whereas for Trumpler 14 the limiting magnitudes are $U = 19.9, B = 20.1, V = 19.1, R = 18.0$ and $I = 20.5$. As for Collinder 232, we compare our photometry with previous ones. Since recent studies usually provide a comparison with the photoelectric photometry by Feinstein et al. (1973), we report here the same comparison. Based on this, comparisons with other photometric studies can be quickly performed.

For Trumpler 14 (27 stars in common), we obtain

$$V_{CRVP} - V_{FFM} = 0.06 \pm 0.16$$

$$(B - V)_{CRVP} - (B - V)_{FFM} = 0.02 \pm 0.100$$

$$(U - B)_{CRVP} - (U - B)_{FFM} = 0.06 \pm 0.11$$

whereas for Trumpler 16 (44 common stars), we obtain

$$V_{CRVP} - V_{FFM} = 0.04 \pm 0.12$$

$$(B - V)_{CRVP} - (B - V)_{FFM} = 0.04 \pm 0.04$$

$$(U - B)_{CRVP} - (U - B)_{FFM} = 0.06 \pm 0.13$$

where the suffix FFM refers to Feinstein et al. (1973) photometry.

The CMDs for all the measured stars are plotted in Fig. 5 and Fig. 6 for Trumpler 14 (343 stars) and Trumpler 16 (1100 stars), respectively. In the case of Trumpler 14, our photometry reaches $V = 19$, and is as deep as that presented by Vazquez et al. (1996). As for Trumpler 16, our photometry reaches $V = 21$, two magnitudes deeper than the study of DeGrijs-Eastwood et al. (2001). The same kind of comments as for Collinder 232 CMDs can be done both for Trumpler 14 and 16. The Main Sequence (MS) is well defined for almost all its extension, but below $V = 17 - 18$ the scatter in color is quite large. This is mostly due to background star contamination, and only partially to photometric errors and the presence of unresolved binary systems, whose percentage in these

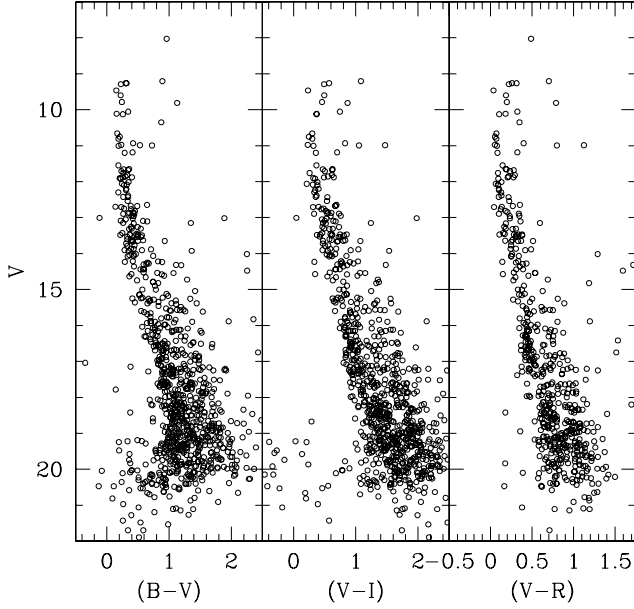


Fig. 6. The CMDs of Trumpler 16 including all the detected stars.

clusters is also around 30% (Levato et al 1990).

In the case of Trumpler 16, the data completeness (V magnitude) analysis provides 100% down to $V=17.4$, 91% down to $V=18.6$ and 57% down to $V=19.3$. As for Trumpler 14, we find 100% down to $V=16.9$, 89% down to $V=17.4$ and 51% down to $V=18.1$.

6. The interstellar extinction toward

Collinder 232, Trumpler 14 and Trumpler 16

The Carina region is characterized by a remarkable concentration of young stars (it contains a sizable fraction of the known OB stars of the Galaxy; Walborn, 1995; Tapia et al. 2003), and gas (the large H II region NGC 3372). As shown in Figure 1, the interstellar medium appears to be very clumpy and great care should be taken to treat the interstellar extinction properly, as it is not possible to adopt a unique average extinction law over the whole region (see also The & Graa and, 1995). Tapia et al. (2003) do not perform a new analysis of the problem, but simply adopt previous findings by Tapia et al. (1988), Smith (1987) and results presented at the 1995 La Plata workshop on Carina (1995, Rev. Mex. Astron. Astrof. 2).

Here we analyse this issue in a completely new fashion, and tackle the problem of variable extinction by first deriving the appropriate law for each cluster, and then applying it to deredden the individual stars in each of them.

6.1. The reddening laws

In order to estimate the selective extinction $R_V = A_V = E(B-V)$ toward each cluster, we combine our UV-optical UBVR photometry with the near-IR one in the JHKL bands from Tapia et al (1988) and the spectral classification from Levato & Malaroda (1982) and Morrell et al (1988). The comparison between the measured and intrinsic colours expected for the stars' spectral type (Wegner 1994) allows one to compute the colour excesses in the different bands and, ultimately, R_V . To do so, we have applied three different methods and compared the results:

(i) The first method is based on the following approximate relation (e.g. Wittet, 1992):

$$R_V \approx 1.1 \frac{E(V-K)}{E(B-V)} \quad (5)$$

which relies on the fact that, as the wavelength increases, the reddening law becomes less dependent on the nature of the dust grains and, hence, the ratio between absorption in the V and K band is nearly a constant along different lines of sight. Its weak point, though, is that it only uses the flux in two spectral regions, and not the entire extinction curve.

(ii) The second method we employ partially overcomes this limitation by using the extinction curve redwards of the R band, but requires its shape to be known a priori (Morbidelli et al, 1997; Patriarchi et al 2001; see also Carraro, 2002 for an application to Trumpler 15).

First, A_V is determined with a least-square fit to the following relation:

$$E(B-V) = A_V (R_L(B-V) - 1) \quad (6)$$

where $R_L = R; I; J; K; L$ and R_L is the extinction curve $A_\lambda = A_V R_L(\lambda)$. We have adopted the one from Rieke & Lebofsky (1985). Then, R_V is computed from the measured $E(B-V)$ and the value of A_V derived above.

Since the fitting equation 6 is a homogeneous one, the uncertainty on A_V for each input star has been computed by considering $N-1$ degrees of freedom, N being the number of photometric bands available. This implies that we can obtain only a lower limit on the R_V uncertainty, since it is rather difficult to take into account spectral misclassification and, hence, inaccuracy in the adopted intrinsic colors (Patriarchi et al 2001).

(iii) In the third and last method the information in all the available passbands is used. In addition, no assumptions are made on the extinction law, but, rather, R_V is derived by extrapolating the extinction curve to infinite wavelengths:

$$R_V = \lim_{\lambda \rightarrow \infty} \frac{E(B-V)}{E(V-\lambda)} = E(B-V) \quad (7)$$

under the (obvious) assumption that:

$$\lim_{\lambda \rightarrow \infty} A(\lambda) = 0 \quad (8)$$

In practice, the measured values of $E(V - I) = E(B - V)$ in the available bands are fitted with a 5th order polynomial, which is then extrapolated to $1 - I = 0$. The linear term in the polynomial is set to 0 to ensure that the extrapolated curve is horizontal at the limit.

In addition to R_V this method also yields the complete reddening curve. While R_V differs significantly from star to star (see Tables 5, 6 and 7 for Trumpler 14, Collinder 232 and Trumpler 16, respectively), the shape of the reddening curve shows, within the accuracy of our measurements, no significant variations and follows closely the one by Rieke & Lebofsky (1985). Therefore, in the following we will adopt it, scaled to the appropriate values of R_V , to deredden our target stars.

The results for R_V are summarized in Tables 5, 6 and 7 for Trumpler 14 (10 stars), Collinder 232 (3 stars) and Trumpler 16 (14 stars), respectively. There, the stars' identification is reported together with the individual reddening $E(B - V)$, the value of R_V as obtained with methods (i), (ii) and (iii) and the total absorption A_V derived from the method (ii).

The mean A_V for Trumpler 14 and 16 turn out to be 2.0 ± 0.13 and 1.84 ± 0.65 , and are consistent with the values reported by Tapia et al. (2003).

Even by a cursory inspection of these Tables, it is clear that there are large variations in R_V not only from cluster to cluster, but also from star to star within the same cluster.

In Table 8, we finally report for each cluster the adopted mean value of R_V from the three different methods, as obtained by performing an arithmetic mean through the data listed in Table 5 to 7.

Table 8 is very useful to compare the R_V values obtained from different methods. It appears that the methods (i) and (iii) produce comparable results, whereas method (ii) has a tendency to provide lower values of R_V . The only case for which all the 3 methods yield the same result is the case of Trumpler 16, for which the number of stars is the largest one. This immediately raises the suspect that all methods probably would yield comparable results, when a sufficient number of stars were available. Obviously, this hypothesis needs to be validated.

Nonetheless, since all these three methods have pro and contra, we opted for the adoption of individual cluster R_V s estimated by extracting a weighted mean of the three methods. These values are reported in the last column of Table 8 together with the weighted errors. In the case of Collinder 232 the reported error is artificially small, being the statistics very poor.

Trumpler 14 has the largest value of R_V and Trumpler 16 the lowest one, with Collinder 232 in the middle, both in the mean value and in the individual determinations.

The value $R_V = 4.16 \pm 0.07$ we obtain for Trumpler 14 is in good agreement with the one found by Vazquez et al. (1996) using a variety of methods. Finally, we note that

Table 8. Estimates of R_V for the clusters under study.

Cluster	R_V (i)	R_V (iii)	R_V (ii)	Adopted				
Trumpler 16	3.69	0.55	3.45	0.69	3.31	0.51	3.48	0.33
Trumpler 14	4.47	0.48	4.18	0.42	3.81	0.49	4.16	0.21
Collinder 232	4.13	0.25	3.82	0.10	3.46	0.14	3.73	0.03

the relation we find between Trumpler 14 and 16, i.e. $R_V(\text{Tr}14) = R_V(\text{Tr}16) + 0.68(\pm 0.20)$, is only in marginal agreement with the one by The & Graa and (1995).

Regrettably, the paucity of data available for Collinder 232 does not allow one to draw any firm conclusions on the behaviour of the dust in it. What we can say, however, is that R_V is definitely different from Trumpler 14 and 16, independently of the claim that Collinder 232 is not a real cluster, but, rather, its stars belong to either of its two neighbors.

6.2. Individual reddenings and membership

In the previous section we have determined the appropriate extinction curve for every cluster, i.e. the one from Rieke & Lebofsky normalized to the values of R_V listed in the last column of Table 8. We can now use it, together with our UBVR I photometry, to deredden all the stars we have detected in the three clusters. To do so, we have applied the technique developed by Romaniello et al (2002). In brief, given a reddening curve and a set of stellar atmosphere models (the ones by Bessel et al 1998, in our case), the extinction coefficients and intrinsic magnitudes are computed as a function of the effective temperature (and, in the case of the absorption coefficients, also optical depth). The models are, then, reddened by different amounts of $E(B - V)$ and a χ^2 technique is applied to determine the best combination of T_{eff} and $E(B - V)$ for every star. The results are discussed in details in the next Section.

7. Clusters parameters

7.1. Distances

The clusters distances have been calculated by superimposing the observed points to an empirical Main Sequence (MS). Particular care was taken to fit the upper part of the diagram, which is populated by intermediate and high mass stars, for which we may assume, due to the rapidity of their pre-MS evolution, that the Zero Age MS corresponds to the observed MS. In performing the fit we paid attention to reproduce the bulk of the stars simultaneously in 3 CMDs (B_0 vs $(U - B)_0$, V_0 vs $(B - V)_0$, I_0 vs $(V - I)_0$) and in the HR diagram, which are presented in Figs. 7, 8 and 9 for Trumpler 14, Collinder 232 Trumpler 16, respectively. This strategy is mainly motivated by the almost vertical shape of the MS in the V_0 vs $(B - V)_0$, which alone prevents reliable conclusions on the distance of any star cluster, and takes

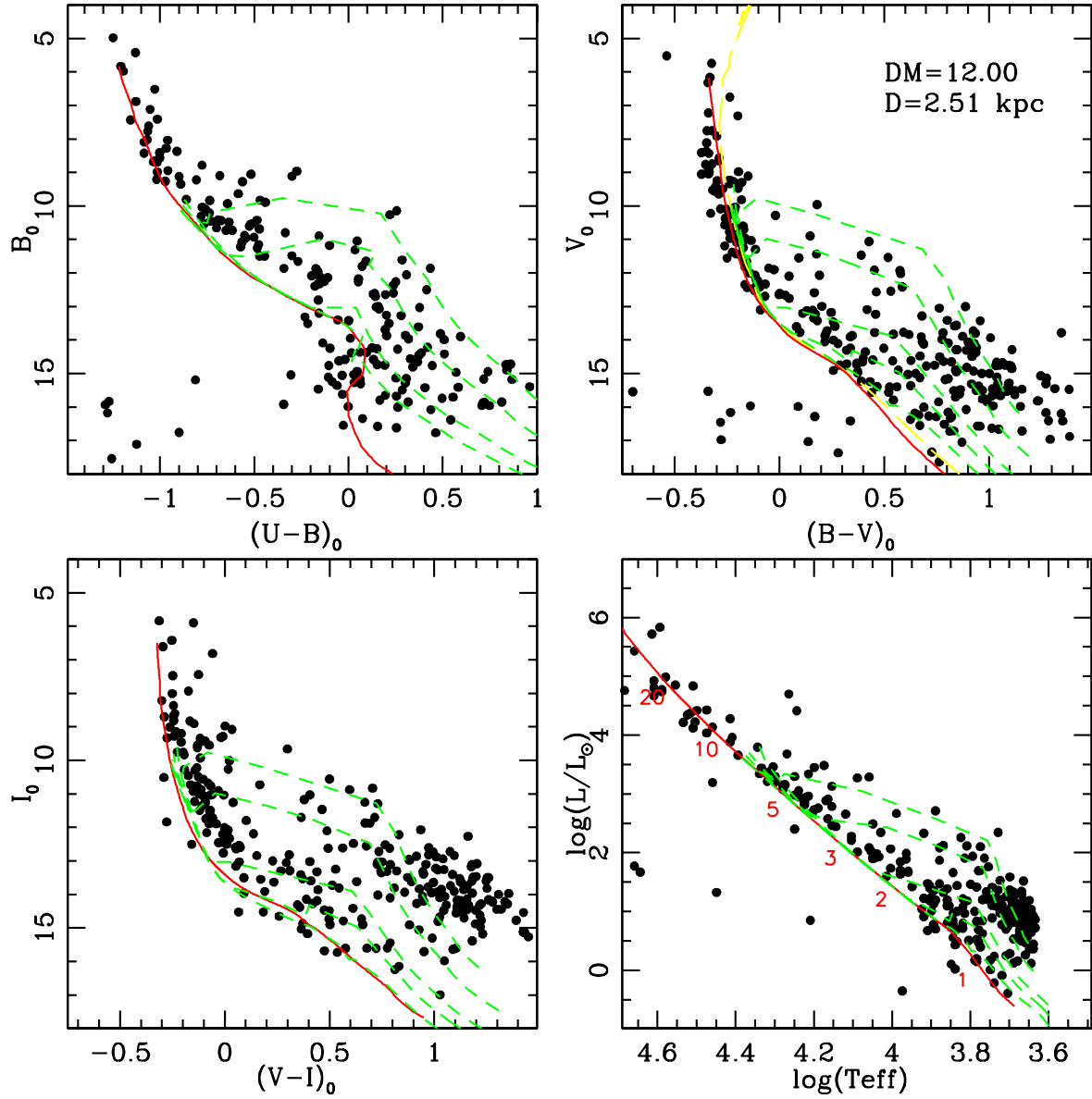


Fig. 7. CMDs and HR diagram for the stars in the field of Trumpler 14. Dashed lines are pre-M S isochrones from Ventura et al. (1998) for the ages of 0.5, 1, 5, 10 and 20 million years. The solid line is an empirical ZAMS. In the HR diagram the number along the sequence indicate the star masses.

full advantage of the more favorable shape of the U_0 vs $(U-B)_0$ and HR diagrams.

Another point to be emphasized is that we did not perform a membership selection for all the clusters. This is due to the fact that proper motions from Cudworth et al. (1993) are available only for stars brighter than 15 mag in V , where the contamination of field stars is less severe, and also to the fact that we are actually covering the inner regions of the three clusters. This does not mean that we are going to consider field star contamination ineffective. Only, we believe that field star contamination does not alter our analysis and conclusions significantly (but see the discussion below). However, we do cross-correlate our Trumpler 16 data with Cudworth

et al. (1993) one, in order to clean the upper part of the M S, which in the case of this cluster is rather blurry. This fact not only helps us to better constrain the cluster distance, but also to clarify whether the cluster is actually somewhat older than the other two.

Trumpler 14 (Fig. 7) We find a good agreement between the observed and the theoretical sequences in the four aforementioned planes for Trumpler 14 by shifting the ZAMS by $(m-M)_0 = 12.3 \pm 0.2$ (error by inspection), which implies a distance of 2.5 ± 0.3 kpc from the Sun. We notice that this value is in perfect agreement with the study by Vazquez et al. (1996, $(m-M)_0 = 12.5 \pm 0.2$, error also here by inspection), where a detailed analysis

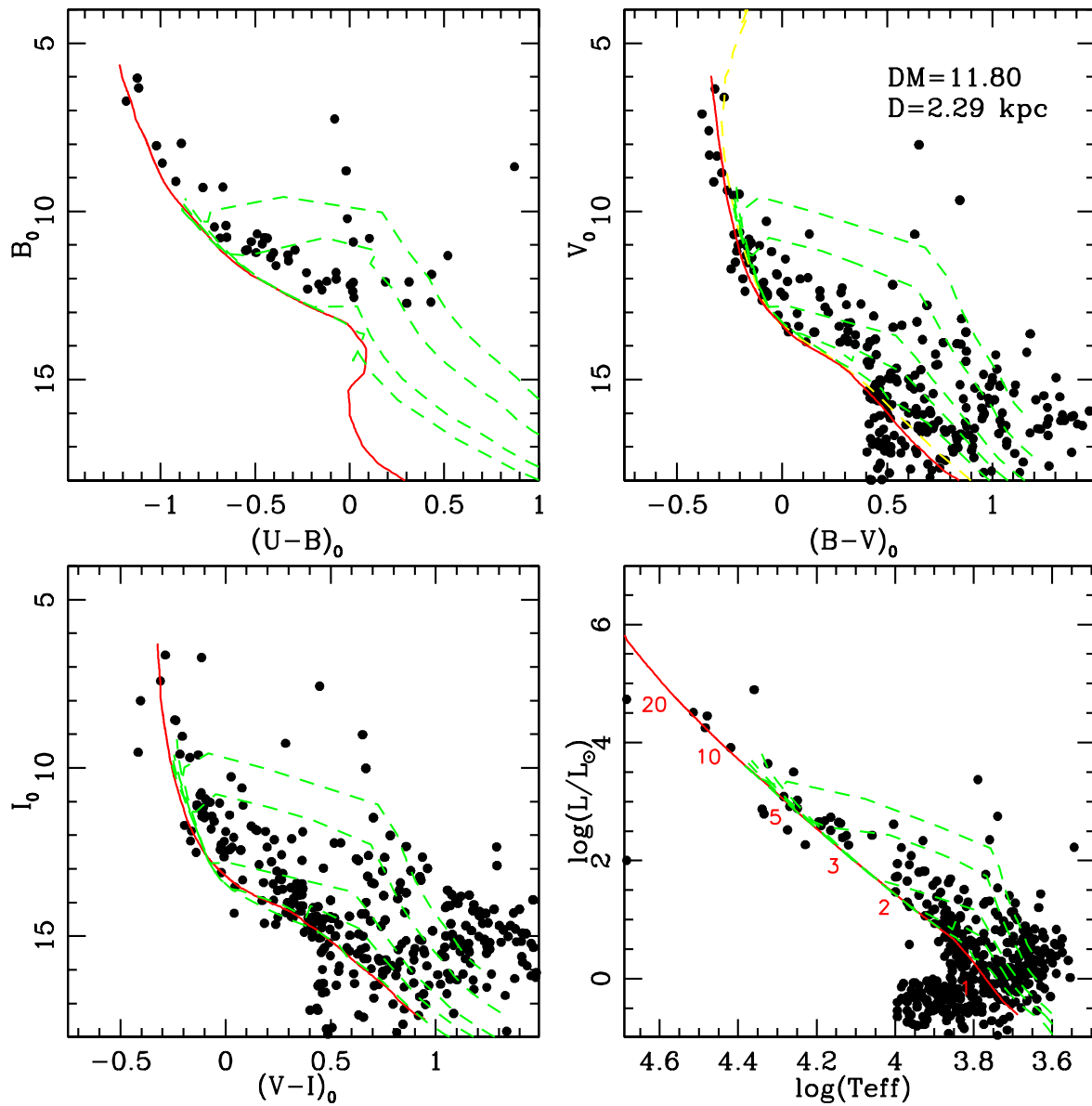


Fig. 8. CMDs and HR diagram for the stars in the field of Collinder 232. Dashed lines are pre-M S isochrones from Ventura et al. (1998) for the ages of 0.5, 1, 5, 10 and 20 million years. The solid line is an empirical ZAMS. In the HR diagram the number along the sequence indicate the star masses.

of the reddening has been done as in our case, but with a different technique. Tapia et al. (2003) finally find $(m - M)_0 = 12:23 \pm 0:67$, again in perfect agreement with our findings. This result gives us much confidence when dealing with clusters (like Trumpler 16, see below) where the field stars contamination is more severe.

Collinder 232 (Fig. 8) We find a good agreement between the observed and the theoretical sequences in the four diagrams for Collinder 232 by shifting the ZAMS by $(m - M)_0 = 11:8 \pm 0:2$ (error by inspection), which implies a distance of $2:3 \pm 0:3$ kpc from the Sun. Basically, Collinder 232 is almost at the same distance as Trumpler 14. The CMDs of Collinder 232 show the same

features of those of Trumpler 14 and 16 (see below), thus suggesting the possibility that this cluster is probably a physical one.

Trumpler 16 (Fig. 9 and 10) The situation for Trumpler 16 is somewhat more complicated, since the cluster is much more heavily contaminated by field stars, and the upper part of the MS is rather broad. However, when proper motion members are considered, the situation gets better. Tapia et al. (2003) report a distance $(m - M)_0 = 12:02 \pm 0:57$, and place the cluster at the same distance of Trumpler 14. In the case of Trumpler 16, however, the traditional CMDs V_0 vs $(B - V)_0$ (upper right panel) and I_0 vs $(V - I)_0$ (lower left panel) do not

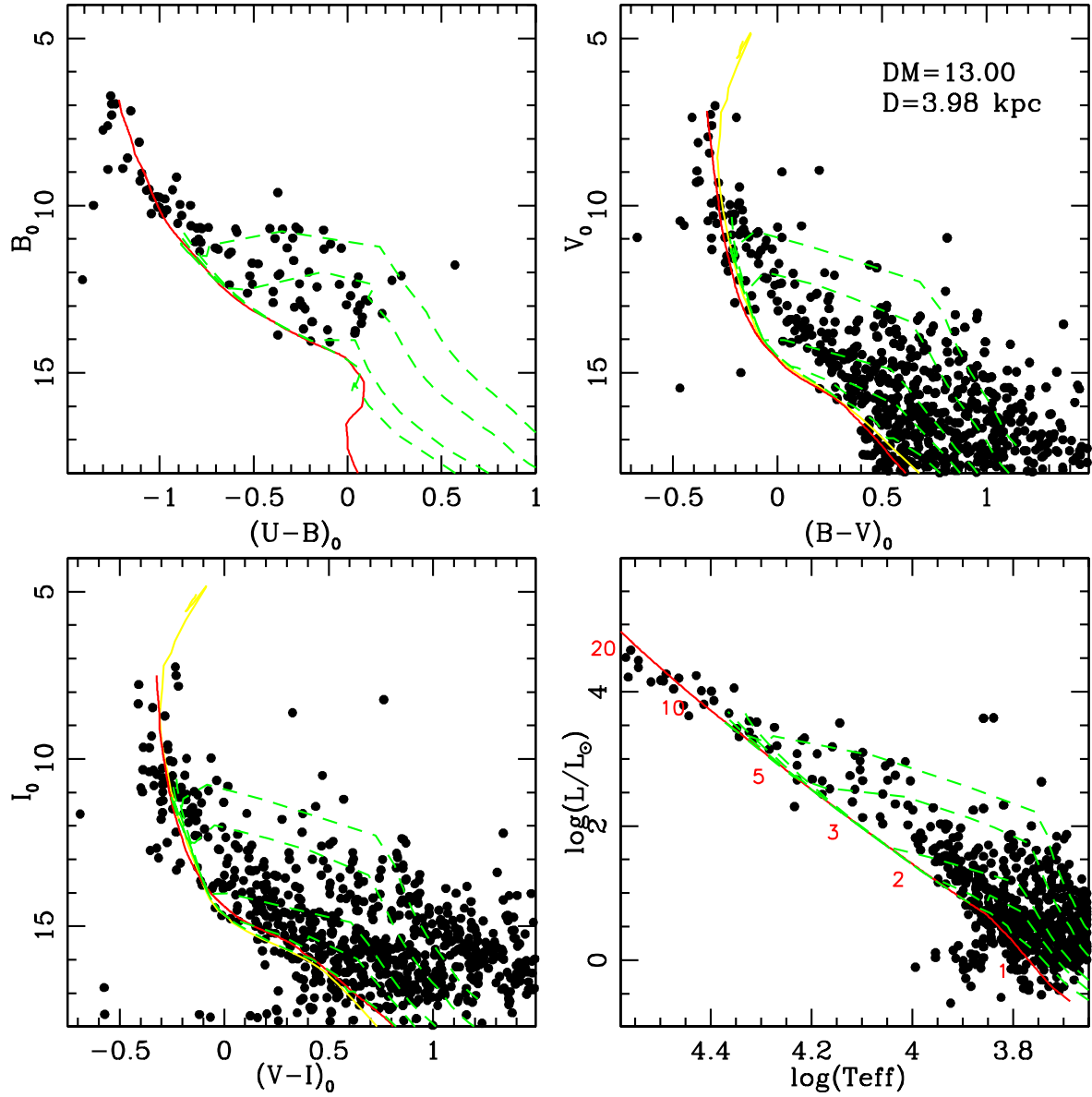


Fig. 9. CMDs and HR diagram for the stars in the field of Trumpler 16. Dashed lines are pre-M S isochrones from Ventura et al. (1998) for the ages of 0.5, 1, 5, 10 and 20 million years. The solid line is the empirical ZAMS shifted by $(m-M)_0 = 13.00$. Finally the dashed line is a 5 Myr isochrone from Girardi et al. (2000). In the HR diagram the number along the sequence indicate the star masses. See text for additional details.

help in finding a reliable value for the distance modulus. In fact, the ZAMS in Fig. 9 and Fig. 10 have been shifted by $(m-M)_0 = 13.00$ (solid line) and 12.00 (dotted line), and do not exhibit any real difference. On the contrary, in the B_0 vs $(U-B)_0$ CMD (upper left panel) and in the HR diagram (lower right panel) they detach much more significantly, and only the larger distance modulus ZAMS provides a good fit of the data (see Fig. 9 and 10). In conclusion, taking advantage of the large colour baseline, we can reach a good fit by shifting the ZAMS by $(m-M)_0 = 13.00 \pm 0.30$ (error by inspection), which in turn yields a distance of 3.98 ± 0.5 kpc. We note that this

value is considerably larger than any previous estimate of the distance of Trumpler 16.

7.2. Ages and age spreads

The age and age dispersion estimate is a cumbersome task. Our theoretical tracks have been calculated by using the ATON 2.0 code for stellar evolution, a full description of which can be found in Ventura et al. (1998). The pre-M S tracks are calculated starting from an extremely cold structure ($\log T_c = 5.7$), and an evolutionary status which takes place before the deuterium burning. This approach can be adopted for the description of the early

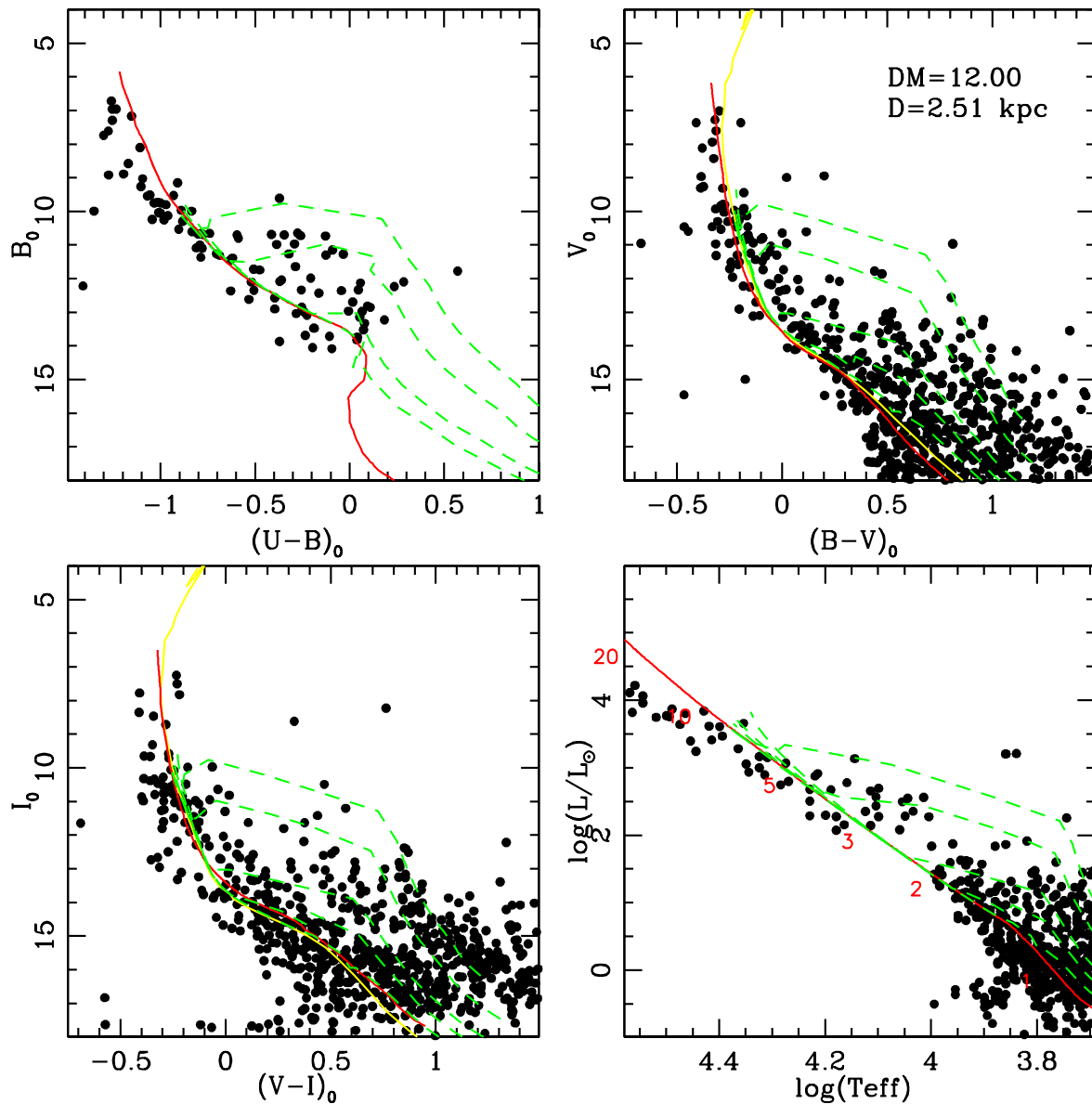


Fig. 10. Same as Fig. 9, but for $(m - M)_0 = 12$. The poor agreement with the data in the $B_0 - (U - B)_0$ and HR diagrams for this distance modulus is apparent.

evolution of low mass stars ($M < 1.5 M_\odot$), but it is inadequate to determine the age of more massive objects, since these latter complete deuterium burning during the accretion phase, which is not taken into account within our hydrostatic framework: for these stars we can only provide an estimate of the time needed to reach the main sequence. We therefore set a minimum age for all the stars populating the MS, while the analysis focused on the determination of the ages of the single stars still in the pre-MS phase was limited to objects with mass $M < 1.5 M_\odot$. As for massive stars, we are going to compare their distribution with post-MS isochrone from Girardi et al. (2000).

Trumpler 14 (Fig. 7) Fig. 7 shows the observed stars of Trumpler 14, along with our theoretical isochrones (Ventura et al. 1998, dashed lines) corresponding to ages of 0.5, 1, 5, 10 and 20 $\times 10^6$ yrs from the bottom to the top. The solid line is an empirical ZAMS, whereas the long-dashed line is a 2 Myr post-MS isochrone from Padova models (Girardi et al. 2000). We note a well populated MS down to $M \approx 2 M_\odot$, with no hints of stars leaving the MS. In the lower part of the CMD and HRD we see that the pre-MS population lies systematically rightward the pre-MS isochrone corresponding to an age of 2 $\times 10^7$ yrs, which can be considered as the maximum age dispersion of the intermediate-mass stars in the cluster. As for the age, since there is no clear indication of massive stars in the act of leaving the ZAMS, we suggest a very

young age (less than 2 Myr) for Trumpler 14, in perfect agreement with previous suggestions (Vazquez et al. 1996).

Collinder 232 (Fig. 8) The situation concerning Collinder 232 is much better defined. As in the case of Trumpler 14, we note a homogeneously populated MS down to masses $M \approx 2M_{\odot}$, and a population of pre-MS stars in the lower part of the diagram well detached from the theoretical MS. We have therefore indications from photometry that Collinder 232 is indeed a physical group, and we find that the dispersion of the ages is again within 2×10^7 yrs. As for the age, the same kind of comments as in the case of Trumpler 14 (see above) can be done.

Trumpler 16 (Fig. 9) The analysis for Trumpler 16 is much more complex because the upper MS is larger. Since we are taking only proper motion members into account, the width of the upper MS has to be considered as due to the presence of massive stars out of the MS, which in turn implies that this cluster is older than Trumpler 14. To clarify this issue, in Fig. 9 we have drawn also a post-MS isochrone from Girardi et al. (2000) for the age of 5 million years, which provides a reasonable fit to the data, in the sense that there is the evidence that even somewhat less massive stars are in the act of leaving the MS.

Besides, in the lower part of the diagram it is not completely clear which stars effectively belong to the cluster, so that the dispersion of the ages is extremely hard to define. The proximity of stars in the lower part of the diagram to the MS seems to indicate a further older low mass stars population, but this conclusion is made very uncertain by the tentative knowledge of the effective membership of the faintest stars.

8. Discussion and conclusions

The main motivation of this study was to clarify the nature of the star aggregate Collinder 232, i.e. whether this is a physical cluster or not, and to investigate the relationship of the cluster with the other two main clusters in the Carina spiral feature, namely Trumpler 14 and 16. We have addressed these issues by analyzing homogeneous photometry in the optical passbands for all the clusters. The first step has been to study the extinction pattern. In analogy with some previous investigations we find that all the clusters are affected by absorption in quite a different way, and that it is not possible – as in some previous studies – to adopt the same reddening law for the entire Carina region. Actually, even assuming the same absorption law within a given cluster could be already a rather crude approximation.

The second step was to derive individual reddening, luminosity and effective temperature for each star inside a cluster. We derived these quantities by employing the method recently developed by Romaniello et al. (2002). Then we analyzed several CMDs and the HR diagram and obtained estimates of the age, age spread and distances.

8.1. Main conclusions

In Table 9 we summarize the main findings of this study. The extinction toward these clusters is highly patchy, a fact not always properly taken into account in previous investigations. Moreover, the analysis of the CMDs of Trumpler 16 reveals that this cluster is significantly detached from the other two clusters and located further away along the Carina spiral arm. This result apparently contradicts previous findings. All three clusters contain a substantial pre-MS population, whose precise membership and consistency however is hampered by field stars contamination. In addition, we find for all the clusters age spreads amounting at most at 20 million years and Trumpler 16 seems to be older than Collinder 232 and Trumpler 14.

8.2. Is Collinder 232 a physical aggregate?

Tapia et al. (2003) performed star counts in the field of Collinder 232, and concluded that there is no cluster there, simply because the star density profile is almost flat and close to the mean field star density in this region. However, they do not consider the appearance of the various CMDs, whose detailed scrutiny reveals that we are facing a population of young stars, as in the case of Trumpler 14 and 16. In other words, the shape of the stars distribution in the CMD is that of a young stellar population, and indeed (see Fig. 1), the main feature of Collinder 232 is a sparse grouping of bright stars. We cannot however simply exclude that Collinder 232 is just part of Trumpler 14 halo. In fact the eastern side of Trumpler 14 (see Fig. 1) toward Collinder 232 is much less obscured than the western part, where the Great Carina nebula is optically very thick. However it is not clear why we should see this bright stars concentration only eastward of Trumpler 14, and not, for instance, northward or southward. The hypothesis of Collinder 232 being part of Trumpler 14 would also be somewhat corroborated by the conclusion of Cudworth et al. (1993) study, that the most probable members of Trumpler 16 are enclosed with a circle 4 arcmin large, which is depicted in Fig. 1, and therefore Collinder 232 is not expected to be part of Trumpler 16. In this respect, Vazquez et al. (1996) report for Trumpler 14 a radius of 2.5 arcmin, to sm all for Collinder 232 being part of Trumpler 14.

We therefore propose the possibility – which further studies should better investigate – that Collinder 232 is a rather sparse, bright stars dominated, young open cluster.

8.3. The Star Formation History in the Carina region

According to Walborn (1995) and Meech et al. (1996) SF is still active in the Carina region. The analysis of Trumpler 14 and 16 lead DeGioia-Eastwood et al. (2001) to conclude that intermediate-mass stars started forming about 10 Myr ago, whereas high mass stars formed only in the last 3 Myr.

Table 9. Estimates of the fundamental parameter of the clusters under investigations.

Cluster	E(B - V)		(m - M) ₀		Distance kpc	Age Myr	Agespread Myr	
	mag	mag	mag	mag				
Trumpler 16	0.61	0.15	13.00	0.30	3.9	0.5	5	20
Trumpler 14	0.57	0.12	12.00	0.20	2.5	0.3	2	20
Collinder 232	0.48	0.12	11.80	0.20	2.3	0.3	2	20

Here we address a different issue, whether the SF in this region has been sequential or not, following Feinstein (1995) terminology. We put together the results of our series of papers (Carraro et al. 2001, Patat & Carraro 2001, Carraro & Patat 2001, Carraro 2002, Baume et al. 2003 and the present one), where a homogeneous data set has been presented and analyzed to derive in a homogeneous fashion the ages of the young clusters in the Carina region listed in Feinstein (1995, Table 1).

We notice that the youngest aggregates are Trumpler 14, Collinder 232 and Trumpler 16, which are located in the core of the region. A bit further away, along the southern and northern extension of the arm, there are NGC 3324 (same age as Trumpler 16), Trumpler 15 (6 Myr), Collinder 228 (8 Myr) and Bochum 11 (4 Myr), which are also somewhat older. NGC 3293 (10 Myr) and NGC 3114 (300 Myr), located in a most peripheral zone, are again somewhat older. Finally, Bochum 9 and 10 are probably not physical clusters, Collinder 234 seems to be part of Trumpler 16, and VdB-Hagen 99 and Carraro 1 are not related with the Carina spiral feature.

In other words a clue emerges of a shallow age gradient along the spiral arm, which seems to imply that SF started outside the Carina region proceeding toward the core. This basically confirms the suggestions made by Feinstein (1995).

Acknowledgements. The authors deeply thanks the anonymous referee for the her/his encouraging and detailed report who helped a lot to improve on the presentation of the paper. G.C. acknowledges kind hospitality from ESO and Rome Observatory, and very fruitful discussions with Gustavo Luiz Baume and Guido Barbaro. This study made use of Simbad and WEBDA.

References

- Baume G., Vazquez R.A., Carraro G., Feinstein A., 2003, *A & A* 402, 549
- Bessel M.S., Castelli F., Plez B., 1998, *A & A*, 333, 231.
- Cardelli J.S., Clayton G.C., Mathis J.S., 1989, *ApJ* 345, 245
- Carraro G., Patat F., Baumgardt H., 2001, *A & A* 371, 107
- Carraro G., Patat F., 2001, *A & A* 379, 136
- Carraro G., 2002, *MNRAS* 331, 785
- Collinder P., 1931, *Ld. An.*, 2
- Cudworth K.M., Martin S.C., deGloia-Eastwood K., 1993, *AJ* 105, 1822
- deGloia-Eastwood K., Throop H., Walker G., Cudworth K.M., 2001, *ApJ* 549, 578
- Feinstein A., 1969, *MNRAS* 143, 273
- Feinstein A., 1995, *Rev. Mex. Astron. Astrof.* 2, 57
- Feinstein A., Marraco H.G., Muzzio J.C., 1973, *A & A* 12, 331
- Girardi L., Bertelli G., Bressan A., Chiosi C., 2000, *A & A* 141, 371
- Johnson H.L., 1966, in *Stars and Stellar Systems*, University of Chicago Press, p. 69
- Levato O.H., Malaroda S., 1982, *PASP* 94, 807
- Levato O.H., Malaroda S., Garcia B., Orrell N., Solivella G., 1990, *ApJS* 72, 323
- Massey P., Johnson J., 1993, *AJ* 105, 980
- Megeath S.T., Cox P., Brønfmann L., Roelfsema P.R., 1996, *A & A* 305, 296
- Orbidelli L., Patriarchi P., Perinotto M., Barbaro G., Di Bartolomeo A., 1997, *A & A* 327, 125
- Patat F., Carraro G., 2001, *MNRAS* 325, 159
- Patriarchi P., Orbidelli L., Perinotto M., Barbaro G., 2001, *A & A* 372, 644
- Rieke G.H., Lebofsky M.J., 1985, *ApJ* 288, 618
- Romaniello M., Panagia N., Scuderi S., Kirshner R.P., 2002, *AJ*, 123, 915.
- Schmidt-Kaler, Th., 1982, *Landolt-Bornstein, Numerical data and Functional Relationships in Science and Technology, New Series, Group VI, Vol. 2(b)*, K. Schaifers and H.H. Voigt Eds, Springer Verlag, Berlin, p.14
- Smith R.G., 1987, *MNRAS* 227, 943
- Smith N. et al. 2000, *ApJ* 532, L145
- Tapia M., Roth M., Marraco H., Ruiz M.T., 1988, *MNRAS* 232, 661
- Tapia M., Roth M., Vazquez R.A., Feinstein A., 2003, *MNRAS* 339, 44
- The P.S., G. raa and F., 1995, *Rev. Mex. Astron. Astrof.* 2, 75,
- Trumpler R.J., 1930, *Lick Observ. Bull.* 14, 154
- Vazquez R.A., Baume G., Feinstein A., Pardo P., 1996, *A & A* 116, 75
- Walborn N.R., 1995, *Rev. Mex. Astron. Astrof.* 2, 51
- Ventura P., Zeppieri A., D'Antona F., Mazzino I., 1998, *A & A* 331, 1011
- Wegner W., 1994, *MNRAS* 270, 229
- Whittet D.C.B., *Dust in the Galactic Environment*, Institute of Physics Publishing, Bristol, Philadelphia and New York, 1992.